

# Side-chain liquid-crystal copolymers and elastomers with a null coupling between the polymer backbone and the mesogenic groups

W. Guo, F. J. Davis and G. R. Mitchell\*

Polymer Science Centre, University of Reading, Whiteknights, Reading RG6 2AF, UK  
(Received 22 July 1993; revised 11 November 1993)

The phase behaviour of a series of uncrosslinked and crosslinked side-chain liquid-crystal copolymers is reported. These materials show a reversible nematic–isotropic transition. The two parent homopolymers prepared from the constituent monomers, which differ only in the length of the coupling chain, exhibit, in one case, a preferential alignment of the mesogenic units parallel to the polymer backbone ( $N_{III}$ ) and, in the second case, an alignment of the mesogenic units perpendicular to the backbone ( $N_I$ ). It is shown that it is possible to prepare a random copolymer, in which the competing influences of these two opposing couplings lead to materials that exhibit no preferential alignment of the mesogens with respect to the polymer chain. Such materials exhibit almost zero coupling between the mesogens and the polymer backbone ( $N_0$ ). At this 'null' composition for the elastomer, it is found that the application of a mechanical field can lead to a transition between an  $N_{III}$  nematic phase and an  $N_I$  nematic phase. The coupling between the mesogenic side groups and the polymer backbone can be resolved into the influence of the nematic field and a hinge effect arising from the detail of the chemical architecture of the coupling chain. Using these observations and the results of a mean-field model of the coupling, we show that the 'hinge' effect is some 2.0 to 1.5 times as effective as the 'nematic'-like interaction between the mesogens and the polymer chain in determining the nature of the coupling.

(Keywords: liquid-crystal polymers; coupling; mean-field model)

## INTRODUCTION

Central to the phase behaviour and properties of side-chain liquid-crystal polymers and elastomers is the nature of the coupling between the long-range orientation order of the mesogenic side groups and the configuration of the polymer chain. It is clear from small-angle neutron scattering studies of deuterium-labelled mixtures of side-chain liquid-crystal polymers that the polymer chain exhibits some ordering as a consequence of the orientational order of the side chains<sup>1–6</sup>. This ordering is large for polymer systems that exhibit smectic phases<sup>1–3</sup> and modest when nematic phases are present. In the latter case both parallel and perpendicular alignments of the polymer chains with respect to the mesogenic units have been observed<sup>4–6</sup>. These studies support the basic concepts of the approach pioneered by Warner *et al.*<sup>7,8</sup>, in that a variety of types of nematic phases can exist dependent on the nature of the sign of the coupling between the side chain and the polymer backbone (Figure 1). However, the direct observation of backbone anisotropy via neutron scattering measurements has only been reported for a limited number of systems. In this contribution we shall explore, using an alternative approach, the nature of the coupling between the mesogenic side groups and the polymer chain in a series

of liquid-crystal copolymers for which the parent homopolymers exhibit different signs of coupling between the side groups and the polymer backbone. In particular, we shall utilize crosslinked systems, in which the nature of the coupling may be evaluated through the response of the material to mechanical deformation<sup>9</sup>.

It is clear from previous studies that the nature of the coupling between the polymer backbone and the mesogenic units is strongly dependent on the length and chemical configuration of the coupling chain<sup>9–12</sup>. A series of nematic acrylate-based side-chain polymers showed

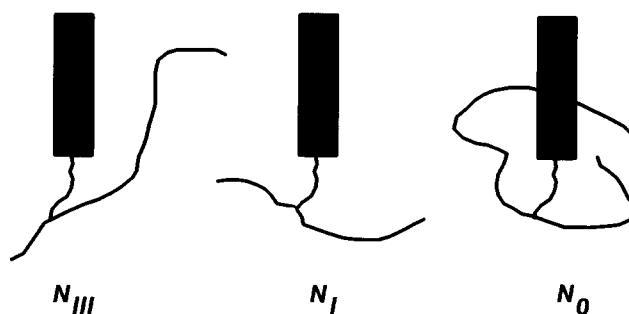


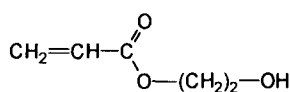
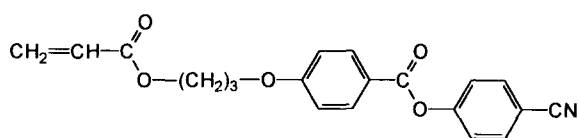
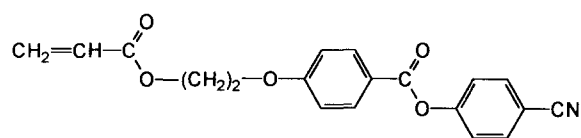
Figure 1 Schematic representation of the types of nematic phases possible in a side-chain liquid-crystal polymer system. The blocks represent the mesogenic units, the lines the polymer backbone and coupling chain

\* To whom correspondence should be addressed

a regular alternation of the sign of the coupling with changing numbers of methylene units in the coupling chain<sup>9</sup>. Similar observations have been made for other polymer systems<sup>13</sup>, and this odd-even dependence is well known from the phase behaviour of low-molar-mass liquid-crystal compounds<sup>14</sup>. A knowledge of the nature and extent of the coupling is vital for an understanding of the fascinating phenomena exhibited by side-chain liquid-crystal polymers and especially elastomers. Effects such as shape changes<sup>15</sup>, memory effects<sup>16</sup>, opto-mechanical transitions<sup>17,18</sup>, shifts in phase transitions<sup>19</sup> and piezoelectricity<sup>20</sup> are all manifestations of the coupling between the mesogenic units and the polymer backbone in side-chain liquid-crystal elastomers.

## MATERIALS

The polymers considered in this work are terpolymers formed using two mesogenic monomers (**I** and **II**) and hydroxyethyl acrylate (**III**), which is used to provide some functionality for subsequent crosslinking<sup>21,22</sup>. The liquid-crystal-forming monomers differ only in the number of alkyl units in the coupling chain. Previous studies of the homopolymers of **I** and **II** show that they exhibit nematic phases, homopolymer **I** giving an N<sub>I</sub> phase (alignment of mesogenic units perpendicular to backbone) and homopolymer **II** an N<sub>III</sub> phase (alignment of mesogenic units parallel to backbone)<sup>9</sup>.



The acrylate mesogenic monomers **I** and **II** were prepared by established routes<sup>21</sup>. The monomer **III** was obtained from Aldrich and distilled under reduced pressure before use. The copolymers were prepared using 10% w/v monomer feedstock in chlorobenzene at 55°C with 1 mol% azobisisobutyronitrile (AIBN) as an initiator. The monomer feedstocks used for each polymerization are tabulated in Table 1. The terpolymers were assumed to have a random distribution of the monomer units within the chains, since more detailed studies of related systems have shown that the kinetics of the polymerization reaction are dominated by the local environment of the radical centre<sup>22,23</sup>. The resulting copolymers were purified by repeated precipitation in methanol/chlorobenzene and dried in vacuum at 55°C for 24 h. The molecular-weight data for these copolymers were obtained using g.p.c. (RAPRA Ltd) with tetrahydrofuran (THF) as the solvent and polystyrene standards. Liquid-crystal elastomers were prepared from a concentrated solution of each of the copolymers in dichloromethane (25% w/v) containing 4% equivalent of monomer repeat units of 1,6-diisocyanatohexane and a small amount of triethylamine (1%) to catalyse the reaction. The solution was cast into a mould formed from Kapton sheeting inside a Petri dish. In order to obtain a bubble-free sample, the cast solution was heated gradually at 55°C for 3 h, 75°C for 16 h, 95°C for 23 h and finally at 105°C for 16 h. This method yielded bubble-free films of 0.1–0.2 mm thickness. Individual samples of 3–5 mm × 10 mm were cut from the large sheet while the sheet was held in the isotropic phase. The basic characteristics of the elastomers prepared in this manner are shown in Table 2.

**Table 2** Characteristics of the elastomers

Elastomer code	Crosslink density from FTi.r. (% repeat units)	Crosslink density from modulus (% repeat units)	Crosslink density from swelling (% repeat units)	T <sub>g</sub> (°C)	T <sub>N<sub>I</sub></sub> (°C)
E3	4.1	1.27 ± 0.13	3.4 ± 0.8	67	100
E81	3.9	1.40 ± 0.13	3.8 ± 1.0	67	99
E72	3.8	1.47 ± 0.30	3.3 ± 0.5	71	100
E63	3.9	1.46 ± 0.13	4.8 ± 1.2	72	99
E55	4.2	1.30 ± 0.13	3.3 ± 0.8	77	102
E2	5.0	1.40 ± 0.13	3.9 ± 0.8	82	102

**Table 1** The characteristics of copolymers

Code	<b>I</b> (mol%)	<b>II</b> (mol%)	<b>III</b> (mol%)	Molecular weight, M <sub>n</sub> (× 10 <sup>4</sup> )	M <sub>w</sub> /M <sub>n</sub> <sup>a</sup>	T <sub>g</sub> <sup>b</sup> (°C)	T <sub>N<sub>I</sub></sub> <sup>b</sup> (°C)	Alignment direction
P3	0	94	6	2.38	3.48	64	101	–
P81	11	83	6	1.87	2.74	65	101	–
P72	23	71	6	1.96	2.61	67	102	0
P63	35	59	6	1.88	3.01	70	102	+
P55	47	47	6	2.19	3.51	74	102	+
P2	94	0	6	2.18	3.56	80	103	+

<sup>a</sup> Obtained from g.p.c. using THF as the solvent and polystyrene standards

<sup>b</sup> Obtained using a Perkin-Elmer DSC with a 20°C min<sup>-1</sup> scanning rate and 5–10 mg samples

## EXPERIMENTAL

*Thermal analysis*

Samples of both uncrosslinked and crosslinked copolymers were examined using a Perkin-Elmer DSC-2 equipped with a workstation to determine the nematic-isotropic phase transition temperatures and the glass transition temperatures. A heating rate of  $20^{\circ}\text{C min}^{-1}$  and a sample weight of  $\sim 5\text{--}10\text{ mg}$  were used for these measurements, and for each sample three successive heating cycles were carried out.

*Optical microscopy*

Samples of the copolymers and elastomers were examined using a polarized light microscope (Carl Zeiss Jenalab) equipped with a Linkam variable hot-stage (TH600) in order to identify the liquid-crystal phase type. Optical micrographs were obtained using a camera fitted on the polarized light microscope.

*I.r. spectroscopy*

The extent of the chemical reactions involved in the crosslinking procedure was evaluated as a function of time using infra-red spectroscopy. In particular, the absorbance of the hydroxy group band at  $\sim 3500\text{ cm}^{-1}$  coupled with the CN band at  $\sim 2230\text{ cm}^{-1}$  enabled the fraction of the reacted hydroxyl units to be obtained, although care had to be taken to eliminate atmospheric moisture. If both functionalities of each diisocyanato-hexane unit react with different polymer chains, then the fraction of reacted hydroxyl units may be equated directly to the crosslink density if intra-chain looping is minimal. Infra-red spectra were obtained using a Nicolet FT-IR and films cast onto KBr substrate. Such films were subjected to the same thermal treatment to induce crosslinking as described in the previous section.

*Modulus measurements*

The mechanical modulus of each elastomer in the isotropic phase was measured using a miniature tensiometer equipped with a variable-temperature oven and a data station. Care was taken to allow adequate time for the sample to reach equilibrium between each strain step, although the timescale of the response was very much shorter than that observed when deforming the same samples in the liquid-crystal state. The modulus  $G$  of the elastomer in the isotropic phase may be related to the crosslink density, or more strictly the molecular weight  $M_c$  between the junction points assuming a perfectly formed network<sup>24</sup>, by:

$$G = RT\rho/M_c \quad (1)$$

where  $\rho$  is the bulk density; here a value of  $1150\text{ kg m}^{-3}$  is used<sup>25</sup>.

*Swelling*

An alternative approach to evaluating the crosslink density is through swelling<sup>24</sup>. The degree of swelling for each elastomer in toluene was determined from the weight of toluene taken up after a period of about 3 h at a temperature of  $70^{\circ}\text{C}$ . The ratio of the volumes of the swollen and unswollen samples,  $q$ , may be related to the average molecular weight between network points by<sup>26</sup>:

$$M_c = \rho V_1 q^{5/3} / (0.5 - \chi) \quad (2)$$

where  $V_1$  is the molar volume of the swelling liquid and

$\chi$  is the Flory-Huggins parameter. The interaction parameter  $\chi$  may be related to the second virial coefficient  $A_2$  by:

$$\chi = 0.5 - A_2 \rho V_1 \quad (3)$$

Equations (2) and (3) may be combined to give:

$$M_c = q^{5/3} / A_2 \quad (4)$$

The second virial coefficient  $A_2$  is not known for any of the present copolymers, although values for a different side-chain system have been reported<sup>27</sup>. We have used for illustrative purposes the value for  $A_2$  of poly(2-ethylhexyl acrylate)<sup>28</sup>. In essence this parameter simply scales the experimental observations onto a crosslink density. The values of crosslink densities obtained for each elastomer are reported in Table 2, and there is broad agreement using the three techniques of i.r. spectroscopy, modulus and swelling that the crosslink densities are similar for each composition. However, the values deduced from i.r. spectroscopy are  $\sim 3$  times those measured from the mechanical modulus. This difference arises from the fact that the spectroscopic approach measures the fraction of reacted hydroxyl sites rather than the number of effective crosslinks. The ratio between these two densities is a measure of the extent of single terminated crosslink units and intra-chain looping. Perhaps not surprisingly, the swelling experiments, although consistent with the other measurements, are clearly different by a constant scale factor. This can be related to the value of the virial coefficient employed. In fact, if we use that obtained by Richtering *et al.*<sup>27</sup>, for a polymer system containing laterally attached mesogenic units, then crosslink densities very similar to those measured through the mechanical modulus are obtained.

*Mechanically induced global orientation*

It is well established that relatively small mechanical extensions applied to 'polydomain' liquid-crystal elastomers can lead to complete global orientation of the liquid-crystal directors<sup>4,9,10,18</sup>. Samples of each elastomer were extended in a miniature tensiometer equipped with an oven at a strain rate of  $\sim 10^{-2}\text{ s}^{-1}$  at fixed temperatures for a range of extension ratios. During the extension, the load, extension and temperature were recorded using a computer system. Each sample was held after deformation at the required extension ratio for about 200 s, before cooling quickly into the glassy state to preserve the orientation pattern imposed during the deformation process.

*X-ray scattering*

Quantitative X-ray scattering measurements were made using a computer-controlled symmetrical transmission three-circle diffractometer equipped with incident beam monochromator and pinhole collimation<sup>10</sup>. Cu K $\alpha$  radiation was used for the experiments, which provide a scattering vector range  $s = 0.2$  to  $6.2\text{ \AA}^{-1}$  ( $|s| = 4\pi \sin \theta / \lambda$ ,  $2\theta$  is the scattering angle and  $\lambda$  the wavelength of the radiation). Intensity data were recorded at points on a grid defined by steps in  $\alpha$  of  $9^{\circ}$  from  $0^{\circ}$  to  $90^{\circ}$  and from  $s = 0.2$  to  $6.2\text{ \AA}^{-1}$  in steps of  $0.05\text{ \AA}^{-1}$ . Here  $\alpha$  is the angle between the extension axis of the sample and the normal to the plane containing the incident and scattered beams. The scattered X-ray intensity data were used to obtain the orientation order parameter for the mesogenic groups  $\langle P_2 \rangle$  where  $\langle P_2 \rangle = \langle 3 \cos^2 \alpha - 1 \rangle / 2$ , using procedures

described elsewhere<sup>29,30</sup>. The scattering functions shown in *Figure 4* are for intensity data that have been fully corrected and scaled using procedures described in detail elsewhere<sup>10,30</sup>.

## RESULTS

### Phase transitions

These copolymers and elastomers all exhibit a reversible nematic–isotropic phase transition. The temperatures observed for this transition for the series of copolymers and the series of elastomers are plotted as a function of the copolymer composition in *Figure 2*. The variation in the phase transition temperature with composition for both crosslinked and uncrosslinked materials is limited. The nematic–isotropic transition temperatures for the elastomer series are found to be 1–2°C lower than for the equivalent uncrosslinked copolymers. The copolymer P2 has a significantly higher glass transition temperature than that displayed by copolymer P3. The glass transition temperatures for the copolymer series (*Figure 2*) are dependent on the concentration of each component present in the material, as expected according to the Fox equation<sup>31</sup>. The glass transition temperatures of the elastomers are about 2–3°C higher than those of the corresponding copolymers, as might be expected.

Earlier experiments<sup>32</sup> performed on melt-drawn fibres of the copolymer series shown in *Table 1* showed that the variation of the copolymer concentration resulted in the nematic phases having a different preferential alignment of the mesogenic units with respect to the polymer backbone. Copolymers containing more than 75% of **II** exhibit an  $N_I$  phase. In this phase, the perpendicular arrangement of the mesogenic units with respect to the polymer backbone arises as a consequence of the negative coupling between the polymer backbone and the mesogenic units. For copolymers with less than 75 mol% of **II**, an  $N_{III}$  phase is observed, with a parallel arrangement between the mesogenic units and the polymer backbone. Such a configuration is the result of a positive coupling between the polymer backbone and the mesogenic units.

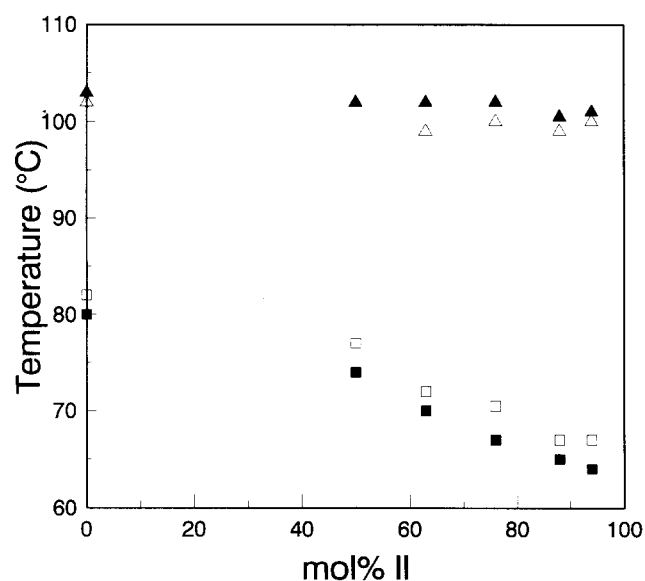


**Figure 2** The glass transition temperature (■, □) and the nematic–isotropic phase transition (△, ▲) as a function of the composition of the material. The full symbols represent the copolymer data and the open symbols the elastomer data

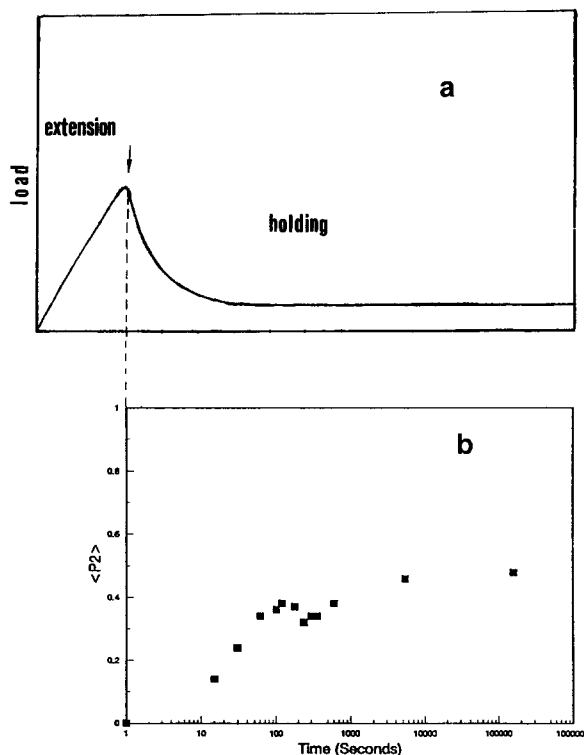


**Figure 3** (a) A plot of the load against time during an extension and holding process for a liquid-crystal elastomer. The position indicated by the arrow is the time at which the extension was stopped. (b) The corresponding orientation parameter  $\langle P_2 \rangle$  measured during the holding period

At the concentration of 75/25 there exists an  $N_0$  phase<sup>32</sup>, in which there is no preferential arrangement between the polymer backbone and the mesogenic units, and hence there is minimal (zero) coupling. The results of these earlier studies in terms of the variation of the nature of the nematic phase with copolymer concentration are also presented in *Table 1*.

### Mechanical induced global orientation

The mechanical properties of the liquid-crystal elastomers in the nematic phase are both strongly temperature- and time-dependent. *Figure 3a* shows a typical time response of the load on the sample. Initially the sample, maintained in this example at 80°C, was continuously extended for 15 s at a strain rate of  $0.013 \text{ s}^{-1}$ . The resultant load rises steeply with extension. Upon ceasing the extension, the load drops in an exponential manner to reach a steady level after  $\sim 100$ – $200$  s. At the extension point corresponding to the peak load the orientation parameter  $\langle P_2 \rangle$  was  $\sim 0$ , indicating no preferred alignment of the liquid-crystal directors. In other words, the drop in load is accompanied by the generation of a monodomain structure, as has been observed in a number of studies<sup>33–35</sup>. The rate of this drop in the load with time is strongly temperature-dependent, and it is particularly influenced by the relative position of the glass transition temperature<sup>34</sup>. We have measured the orientation parameters  $\langle P_2 \rangle$  for samples rapidly cooled to room temperature after holding at a fixed extension for different times. The resultant data are plotted in *Figure 3b*. This shows that the global orientation develops rapidly with time, and reaches a plateau value after some 100 to 200 s. In order to make the reported measurements consistent with such equilibrium conditions, the orientation para-

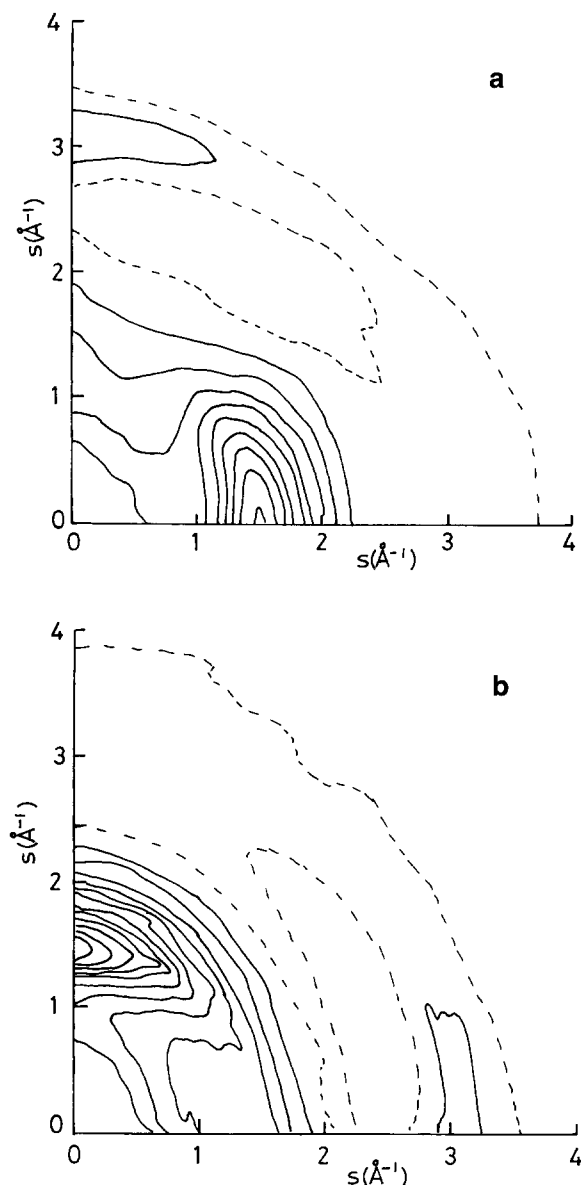


**Figure 4** The X-ray scattering intensity functions  $si(s, \alpha)$  (ref. 10) for samples E2 (a) and E3 (b) at room temperature, which had been subjected to an extension of 1.5 at 85°C and rapidly cooled to room temperature. The extension axis is vertical

meter data presented in this study were obtained for samples that were stretched above room temperature and held in that extension for about 200 s before being rapidly cooled to room temperature. This holding period is sufficient to allow the measured load to reach a steady state.

X-ray scattering measurements were conducted on the glassy deformed samples obtained above. *Figure 4* shows typical X-ray scattering patterns obtained at room temperature for elastomers E2 and E3, after an extension of ~50%. In this study the important feature of these scattering patterns is the arcing of the intense peak at  $s = 1.45 \text{ \AA}^{-1}$ , showing the considerable global anisotropy present in the molecular organization. For E2 (*Figure 4a*) the intensification takes place about the equatorial plane, this is normal to the extension axis. This intense peak arises from the spatial correlations between mesogenic units, and hence intensification is observed normal to the long axes of the side groups. In other words for E2 the

mesogenic units and hence the liquid-crystal directors are aligned preferentially parallel to the extension axis. If we make the very reasonable assumption that the polymer chain is extended preferentially in the extension direction, then the X-ray data show that the mesogenic units lie preferentially parallel to the polymer chain. Similar patterns were also observed for the stretched elastomers E72, E63 and E55. Such a nematic phase was labelled as  $N_{III}$  by Warner *et al.*<sup>7,8</sup>. In *Figure 4b*, an X-ray scattering pattern for elastomer E3 is shown for which the peak at  $s = 1.45 \text{ \AA}^{-1}$  is most intense on the meridional section. This indicates a perpendicular alignment of the mesogenic units to the extension direction. Following the same assumption as above, this pattern indicates a preferred orientation of the polymer chain perpendicular to the liquid-crystal director. Such an arrangement was labelled  $N_I$  by Warner<sup>7,8</sup>.

A quantitative measurement of the global orientation of the mesogenic units can be obtained from the extent of the arcing of the peak at  $s = 1.45 \text{ \AA}^{-1}$  through the orientation parameter  $\langle P_2 \rangle$ <sup>29,30</sup>. *Figures 5* and *6* show plots of the orientation parameter  $\langle P_2 \rangle$  against extension ratio for E2 and E3. These show similar behaviour to that reported for other side-chain liquid-crystal elastomers<sup>9</sup>, in that the global orientation rises with increasing

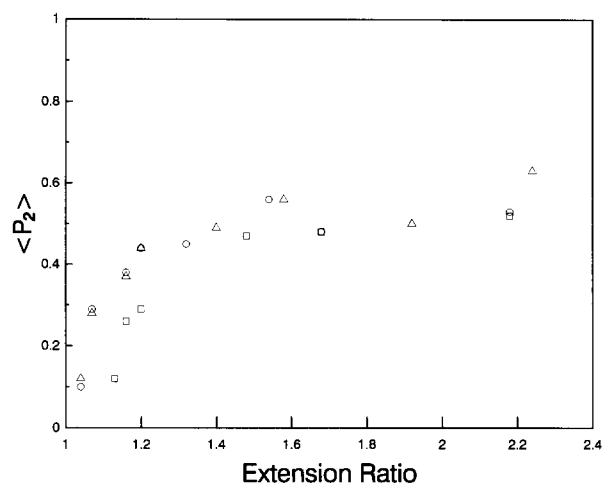


**Figure 5** The orientation parameter  $\langle P_2 \rangle$  against the extension ratio for sample E2 at temperatures of 85°C ( $\square$ ), 90°C ( $\Delta$ ) and 95°C ( $\circ$ )

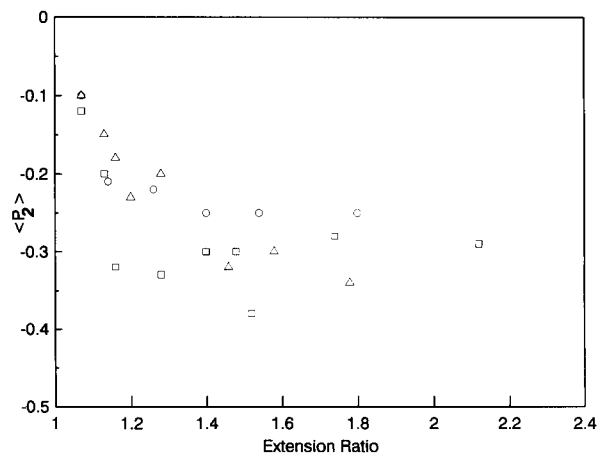


**Figure 6** The orientation parameter  $\langle P_2 \rangle$  against the extension ratio for sample E3 at temperatures of 75°C ( $\square$ ), 80°C ( $\Delta$ ) and 90°C ( $\circ$ )

extension until a plateau is reached at an extension ratio typically around 1.5. It can be noted that as little as 20% deformation in these samples will result in an appreciable global orientation of the mesogenic units with respect to the extension axis. It is also found that there is no observable threshold deformation required to induce a monodomain alignment of the mesogenic units in these elastomers. In a study of liquid-crystal elastomers prepared from the so-called lateral side-chain liquid-crystal polymers, Meier and Finkelmann<sup>36</sup> define a threshold extension that had to be exceeded in order to induce mechanically a global orientation of the liquid-crystal directors. The difference between that observation and the results reported here is the sharpness or breadth of the polydomain–monodomain transition, which may be related to the topology of the network or the nature of the mesogenic units.

We can extract, from the data shown in *Figures 5* and *6*, two parameters that are of particular importance: the first is the plateau orientation parameter; the other is the extension ratio at which the plateau orientation parameter is achieved. The plateau orientation parameter is indicative of the level of preferential alignment in the monodomain structure and is a measure of the liquid-crystal order parameter. The critical extension is a measure of the mechanical extension required for the monodomain alignment to be achieved. This, at least in part, is an indicator of the strength of coupling between the polymer backbone and the mesogenic units. The values of the plateau orientation parameter and the critical extension, which are plotted in subsequent figures, represent averages of the data shown in *Figures 5* and *6*. Typically the uncertainty in these values was  $\pm 0.05$ .

In *Figure 7* the plateau orientation parameters  $\langle P_2 \rangle$  measured for the series of elastomer samples are plotted as a function of the composition of the elastomers. This figure shows more clearly the fact that both the direction and the level of alignment of the mesogenic units are dependent upon the composition of the elastomer. By increasing the proportion of the E3 component in the material, the plateau orientation parameter decreases somewhat, until the concentration of the E3 in the elastomer is  $\sim 83$  mol%, at which composition the global orientation parameter is virtually zero. Upon further increase in the concentration of E3 in the elastomer,

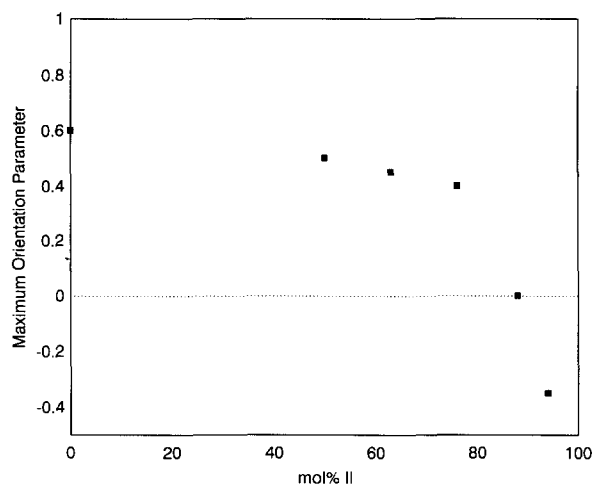


**Figure 7** The plateau orientation parameter  $\langle P_2 \rangle$  against the composition of the elastomer series

the orientation direction changes to the perpendicular arrangement and the orientation level recovers. The phase where no global orientation is observed after stretching is, for convenience, defined as  $N_0$ <sup>32</sup>. Clearly the composition at which the  $N_0$  phase will be observed must be very close to 83% of **II**. Examination of the extent of orientation in X-ray diffraction patterns obtained for melt-drawn fibres of the uncrosslinked copolymers

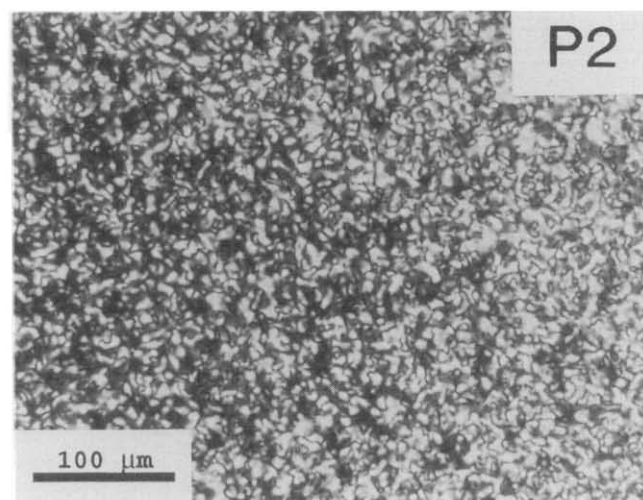
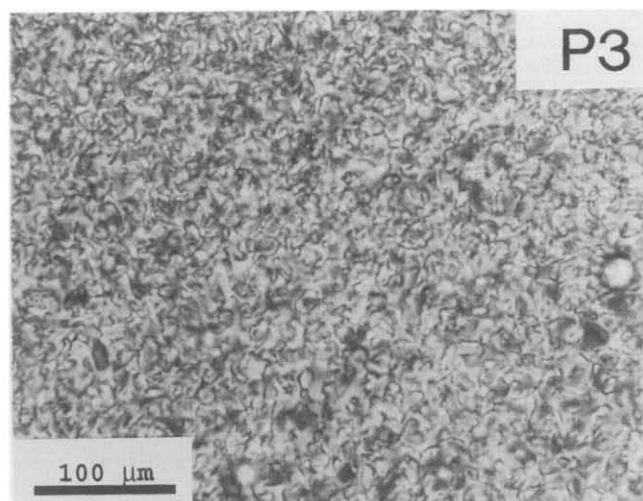
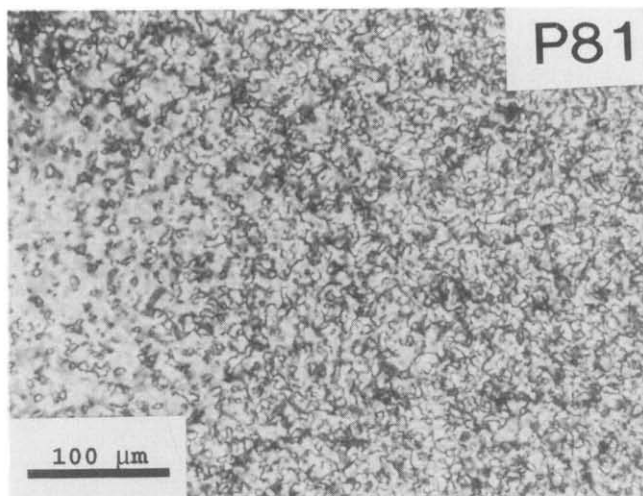


**Figure 8** Optical micrographs of the copolymers P2, P3 and P81 in their liquid-crystal phases showing typical nematic textures

indicated the presence of an  $N_0$  phase at a concentration of about 75% E3<sup>32</sup> as presented in Table 1. The observation of zero global alignment in the elastomer E81 even after substantial mechanical alignment could arise from the absence of liquid crystallinity in the material. Inspection of the optical micrographs for samples of the copolymers P2, P3 and P81 (Figure 8) shows that they all exhibit a threaded texture typical of nematic liquid crystals. The level of birefringence and the nature of the texture for each of these samples is very similar, indicating that the composition of the copolymer in terms of the two mesogenic monomers has not affected the local liquid-crystal structure of the materials.

Figure 9 shows the effect of the elastomer composition on the critical extension ratio required to achieve the plateau orientation at a temperature  $\sim 13^\circ\text{C}$  above the glass transition for each elastomer. It can be seen that the critical extension ratio required increases as the fraction of the E3 component in the elastomer increases. There is a marked divergence at a fraction of  $\sim 83\%$  of E3. Since there is no marked variation in the degree of crosslinking, the change of the critical extension ratio with the concentration demonstrates that the overall

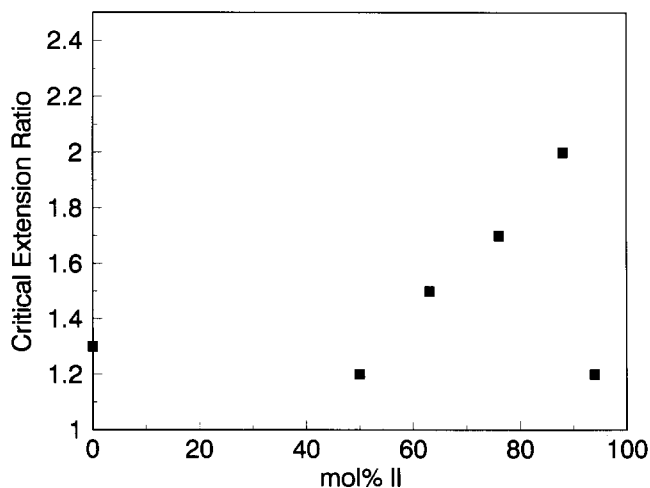


Figure 9 A plot of the critical extension ratio required to achieve a monodomain structure against the composition of the elastomer system

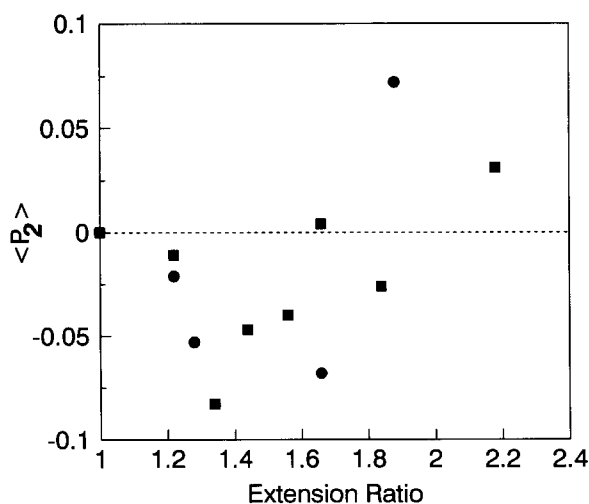


Figure 10 The orientation parameter  $\langle P_2 \rangle$  against the extension ratio for the elastomer E81 at temperatures of  $85^\circ\text{C}$  (●) and  $90^\circ\text{C}$  (■)

coupling between the polymer backbone and the mesogenic units is strongly concentration-dependent.

For the elastomer E81, although there is no major orientation of the liquid-crystal directors upon mechanical extension, the applied mechanical field leads to changes in the alignment direction of the mesogenic units. A plot of the orientation parameter  $\langle P_2 \rangle$  against the extension ratio for the elastomer E81 is shown in Figure 10. It should be noted that the orientation parameters shown are about 5–10 times smaller than those observed for the elastomers at other compositions, indicating rather insignificant coupling between the mesogenic units and the polymer backbone. Although small, the preferred alignment is found to be perpendicular at low extension ratios typically less than 30%, and parallel at higher extension ratios. This demonstrates that the applied mechanical field induces a change of alignment of the mesogenic units with respect to the extension axis.

## DISCUSSION

We have shown that the parent copolymer of I exhibits a parallel coupling between the mesogenic side groups and the polymer backbone and that the equivalent parent copolymer of II shows a perpendicular coupling. The signs of these couplings are preserved when such copolymers are crosslinked. It is remarkable that such a change in behaviour arises from the relatively small change in the chemical configuration from two alkyl units in the spacer chain to three such units. The level of orientational order appears to be undiminished in the crosslinked copolymers when compared to their uncrosslinked counterparts. By producing an intimate mixture of these differing molecular units of I and II through random copolymerization, it is possible to prepare a system in which the competing couplings cancel. It is interesting in this respect to note that mixtures of the parent copolymers of I and II exhibit both a lower critical temperature and an upper critical temperature and that miscibility in the nematic phase range is very limited<sup>37</sup>. Materials that exhibit this zero coupling may be prepared in uncrosslinked or crosslinked form. However, it is interesting to note that there is a difference in copolymer composition at which the  $N_0$  phase is observed between the copolymer series and the elastomer system. Inspection of Table 2 shows that the crosslink densities of the elastomer series are very similar, and therefore the changes in coupling, as reflected in the variation in the plateau orientation parameter and the critical extension ratio, with concentration are a reflection of the overall changes in the coupling, and do not arise in any significant manner from the presence of a network in the elastomer series.

The existence of the copolymer P72 and the elastomer E81, which both exhibit the  $N_0$  phase, indicates that the resultant coupling between the polymer chain and the mesogenic units in these two materials is minimal. The fact that this zero coupling does not occur at a 50/50 mol% composition indicates that the coupling in the P2 system is stronger than that in the P3 system. This must be a direct consequence of the change in the coupling chain length from two alkyl units to three alkyl units. We have utilized a mean-field model, which follows the work of Warner and others<sup>7,8</sup>, in which the polymer system is represented by two mesogenic units (a and b) and the polymer backbone (c). The potential describing

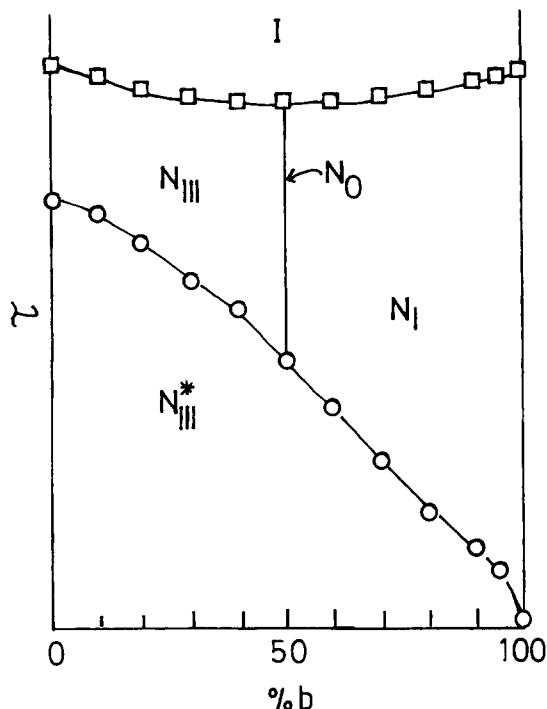


**Figure 11** Phase diagram obtained using the mean-field model described in the text with  $V_{AA} = V_{AB} = V_{Bb}$ ,  $\lambda = 0.5$ ,  $\mu_A = 0.2$ ,  $\mu_B = -0.2$  and  $\tau = k_B T / V_{AA}$ . The symbols indicate the points calculated

the ordering of the polymer chain with respect to the nematic director is given by<sup>38</sup>:

$$H = -P_2[\phi_a \mu_a S_a + \phi_b \mu_b S_b + (1 - \phi_a - \phi_b) \lambda_c S_c] \quad (5)$$

where  $S_{a,b,c}$  are the order parameters for the mesogenic side chain a, mesogenic side chain b and polymer backbone c, respectively,  $\phi_{a,b,c}$  are the fractions of the species in the copolymer,  $\mu_{a,b}$  are the coupling constants between the mesogenic units and the polymer chain,  $\lambda_c$  is the coefficient describing polymer chain–polymer chain interactions and  $P_2$  is the second term in the Legendre polynomial series. These coefficients are expressed as a ratio to the mesogen–mesogen interaction parameter. In the work of Warner *et al.*<sup>7,8</sup>, an additional term relating to the bending of the polymer chain is included. Here, where the polymer chains are very similar and the objective is to examine the effects of changing the mesogen composition, its exclusion will not significantly alter the basic results. Since we are considering random copolymers, the possibility of phase separation is excluded from consideration in this approach. We can use this system to explore the phase behaviour of such random copolymers as a function of composition. *Figure 11* shows such a phase diagram for a system in which the strengths of the coupling coefficients  $\mu_{a,b}$  are set equal in magnitude but opposite in sign. The phase structure is plotted as a function of reduced temperature ( $\tau = kT/V_{aa}$ , where  $V_{aa}$  describes the mesogen–mesogen interactions for the a units). In this case the  $N_0$  phase is observed at the 50/50 composition. It can be seen that there is a drop in the nematic–isotropic transition temperature as the composition approaches the  $N_0$  composition. This drop reflects the contribution of the polymer backbone to the stability of the nematic phase. At high temperatures two nematic phases are observed, an  $N_I$  phase and an  $N_{III}$  phase. At lower temperatures there is a second-order transition from either an  $N_I$  or  $N_{III}$  phase to an  $N_{III}^*$  phase,

which exhibits a highly ordered polymer backbone configuration. The star indicates that the level of order of the polymer backbone is relatively high. Here we have defined the  $N_{III}$  to  $N_{III}^*$  transition at the mid-point or inflection of the polymer chain order parameter  $S_c$  versus  $T$  curve. Of course, this phase with a highly ordered polymer backbone configuration is not accessible with an acrylate-based polymer because of the intervention of the glass transition. By preparing such phase diagrams for differing values of the coupling coefficients  $\mu_{a,b}$ , such calculations<sup>38</sup> show that, for equivalent mesogens, but with opposite sign coupling, the  $N_0$  phase is observed when:

$$\phi = |\mu_a| / (|\mu_a| + |\mu_b|) \quad (6)$$

This is obviously a simplified scheme in which the interactions between the different mesogenic units and each other, independent of the nature of the coupling, are the same. We can equate mesogenic unit a in this model with I and mesogenic unit b with II. This suggests, for the uncrosslinked copolymer series for which  $\phi = 0.75$ , that  $\mu_a = 0.3$  and  $\mu_b = -0.10$  and, for elastomer series for which  $\phi = 0.81$ , that  $\mu_a = 0.45$  and  $\mu_b = -0.10$ . It is emphasized that these are not absolute values but are expressed in relation to the strength of the mesogen–mesogen interaction.

In the approach of Warner *et al.*<sup>7,8</sup> the coupling between the mesogenic units and the polymer chain is composed of two components. The first is that which arises from ‘nematic’-like interactions between the side chain and the polymer chain and which we will label as  $\mu^n$ . The strength of this interaction will depend on the ordering temperature of the polymer backbone<sup>38</sup>. The second component describes the effects arising from the chemical hinge. Arrangements in which the mesogen is forced by stereochemistry, for example, to lie perpendicular to the polymer chain can easily be envisaged. We shall label this effect  $\mu^h$ . In the approach of Warner *et al.*<sup>8</sup> the ‘hinge’ is seen as only offering a negative coupling, and its effect may be varied by altering the density of the mesogenic units along the polymer backbone. We have shown elsewhere by consideration of atomistic models of representative sections of the copolymers that both the sign and the magnitude of the hinge factor depend on the detail of the chemical configuration of the coupling chain, and that both positive and negative hinges are possible<sup>38</sup>. The experiments here suggest that for the uncrosslinked copolymers:

$$\begin{aligned} \mu_a^h + \mu_b^n &= +0.30 \\ \mu_b^h + \mu_a^n &= -0.10 \end{aligned} \quad (7)$$

and that for the crosslinked materials:

$$\begin{aligned} \mu_a^h + \mu_a^n &= +0.45 \\ \mu_b^h + \mu_b^n &= -0.10 \end{aligned} \quad (8)$$

If we make the not-unreasonable assumption that the nematic-like interactions for both mesogenic units are similar in sign and magnitude while the ‘hinge’ effects are similar in magnitude but opposite in sign, then we can deduce that  $\mu^h$  is  $\sim 2$  times  $\mu^n$  for the uncrosslinked copolymers and  $\sim 1.5$  times  $\mu^n$  for the elastomers. The fact that the ratio of  $\mu^h/\mu^n$  obtained for the elastomers is different from that obtained for the copolymer series indicates that the crosslinking has somehow altered the balance of nematic interaction and the ‘hinge’ effects.



A side-chain liquid-crystal elastomer may respond to a mechanical extension through two possible mechanisms. The strain will extend the polymer network and, as a consequence of the coupling, the liquid-crystal directors realign. Recent observations of a strain-induced transition in a monodomain liquid-crystal elastomer sample<sup>39</sup> support the theoretical work of Bladon *et al.*<sup>40</sup>. The latter show that there is a critical extension ratio for director reorientation if the strain is applied normal to the initial director orientation. In that situation, the greater the coupling between the mesogens and the polymer backbone, the greater the critical strain. At other angles the transition is continuous. In a polydomain sample the situation is more complex, but an extension of the approach of Bladon *et al.*<sup>40</sup> to an aggregate polydomain sample shows that there is no critical extension ratio and that in general the rate of macroscopic alignment is inversely related to the degree of coupling<sup>41</sup>. The alternative response of the elastomer is that induced by the stress field, which is coupled into the anisotropy of the mesogenic units. Since the second would only induce an alignment of the mesogenic units along the direction of the stress field, it is logical to say that the first mechanism plays the more important part. This is supported by the observations made on monodomain samples<sup>39</sup>, although the observations here show that the critical strain required to produce a monodomain increases as the coupling decreases, as shown in *Figure 9*. This demonstrates that polydomain samples are more complex. It is highly likely that the shift in the composition at which the  $N_0$  phase is observed from the uncrosslinked series to the elastomers is related to the role of the stress field on the alignment of the mesogenic units. The existence of the  $N_0$  phase is a consequence of the relative balance of opposing interactions, namely, the interaction ( $\mu_{\parallel}$ ) favouring a parallel alignment between the mesogenic units and the polymer backbone, and those interactions ( $\mu_{\perp}$ ) favouring a perpendicular alignment. In the elastomer E81 the interactions  $\mu_{\parallel}$  and  $\mu_{\perp}$  are obviously very similar, hence the balance of these interactions could be changed by the external stress field, as demonstrated by the change of alignment direction of the elastomer E81. In the initial stage of stretching, the stress applied is small and the interaction  $\mu_{\perp}$  is dominant; hence the alignment is perpendicular, as observed for the elastomer E3. However, as the stress field is increased in the later stage of stretching, the original balance is altered and the interaction  $\mu_{\parallel}$  becomes dominant, resulting in a parallel alignment of the mesogenic units with respect to the polymer chain. It is possible that these shifts in the effective coupling coefficients arise from stress-induced conformational changes of the spacer unit.

The transition from the perpendicular alignment to the parallel alignment in the case of elastomer E81 is made possible in the extension range achievable by the small net interactions favouring either parallel and perpendicular preferential alignments. It would not be very surprising if the same transition is obtained for the elastomer E3 at much higher extension ratios than we are able to achieve at the present moment. In effect this would involve a mechanically induced shift in the phase boundary between  $N_I$  and  $N_{III}$  show in *Figure 11* in a similar manner to the shifts observed in the nematic-isotropic phase transition temperatures<sup>18,19</sup>.

This study shows that, for materials that exhibit an  $N_I$  phase, the coupling must be inherently weaker, since the

hinge and the nematic field components of that coupling are in opposition. This has been confirmed in a systematic study of the strength of the coupling as a function of the coupling chain length<sup>9</sup>.

## CONCLUSIONS

In this study we have shown that, for both uncrosslinked and crosslinked copolymers, the nature of the coupling between the polymer backbone and the mesogenic side groups is strongly dependent on the chemical configuration of the coupling chain. Random copolymerization provides a mechanism for generating an intimate molecular mixture of liquid-crystal-forming units whose parent systems exhibit different nematic phases. At a particular composition the competing influences cancel and a material with no effective coupling is generated. Such minimal coupling in the uncrosslinked copolymer series is at a composition of 75/25 mol%, while in the elastomer series such a zero coupling phase is observed at a composition close to 83/11 mol%. At this composition it is found that an applied mechanical field can induce a transition from the initial perpendicular alignment to parallel alignment as the strain applied is increased. Using these observations and the results of a mean-field model of the coupling, it is shown that the 'hinge' effect is between 2 and 1.5 times as effective as the 'nematic'-like interaction between the mesogens and the polymer chain in determining the nature of the coupling.

## ACKNOWLEDGEMENT

This work was supported by the Science and Engineering Research Council (GR/F08405).

## REFERENCES

- Noirez, L., Moussa, F., Cotton, J. P., Keller, P. and Pepy, G. *J. Stat. Phys.* 1991, **62**, 997
- Noirez, L., Pepy, G., Keller, P. and Benguigui, L. *J. Phys. (Fr.) II* 1991, **1**, 821
- Keller, P., Carvalho, B., Cotton, J. P., Lambert, M., Monssa, F. and Pepy, G. *J. Phys. (Fr.)* 1985, **46**, L1065
- Mitchell, G. R., Davis, F. J., Guo, W. and Cywinski, R. *Polymer* 1991, **32**, 1347
- Kirste, R. G. and Ohm, H. G. *Makromol. Chem., Rapid Commun.* 1985, **6**, 179
- Davidson, P., Noirez, L., Cotton, J. P. and Keller, P. *Liq. Cryst.* 1991, **10**, 111
- Wang, X.-J. and Warner, M. *J. Phys. (A)* 1987, **20**, 713
- Warner, M. in 'Side-Chain Liquid Crystal Polymers' (Ed. C. B. McArdle), Blackie, Glasgow, 1989, Ch. 2
- Mitchell, G. R., Coulter, M., Davis, F. J. and Guo, W. *J. Phys. (Fr.) II* 1992, **2**, 1121
- Mitchell, G. R., Davis, F. J. and Ashman, A. *Polymer* 1987, **28**, 639
- Hammerschmidt, K. and Finkelmann, H. *Makromol. Chem.* 1989, **190**, 1089
- Finkelmann, H., Kock, H.-J., Gleim, W. and Rehage, G. *Makromol. Chem. Rapid Commun.* 1984, **5**, 287
- Schatzle, J. and Finkelmann, H. *Mol. Cryst. Liq. Cryst.* 1987, **142**, 85
- Toyne, K. J. in 'Thermotropic Liquid Crystals' (Ed. G. W. Gray), Wiley, Chichester, 1987, p. 28
- Guo, W., Davis, F. J. and Mitchell, G. R. *Europhys. Lett.* in press
- Legge, C. H., Davis, F. J. and Mitchell, G. R. *J. Phys. (Fr.) II* 1991, **1**, 1253
- Guo, W., Davis, F. J. and Mitchell, G. R. *Polymer* submitted

- 18 Schatzle, J., Kaufhold, W. and Finkelmann, H. *Makromol. Chem.* 1989, **190**, 3269
- 19 Davis, F. J. and Mitchell, G. R. *Polymer* submitted
- 20 Meier, W. and Finkelmann, H. *Makromol. Chem., Rapid Commun.* 1990, **11**, 599
- 21 Portugal, M., Ringsdorf, H. and Zental, R. *Makromol. Chem.* 1982, **183**, 2311
- 22 Davis, F. J., Gilbert, A., Mann, J. and Mitchell, G. R. *J. Polym. Sci., Polym. Chem. Edn.* 1990, **28**, 145
- 23 Hirai, A., Mitchell, G. R. and Davis, F. J. *New Polym. Mater.* 1990, **1**, 251
- 24 Treloar, L. R. G. 'The Physics of Rubber Elasticity', Clarendon Press, Oxford, 1975
- 25 Symons, A. J. PhD. Thesis, University of Reading, 1993
- 26 Flory, P. J. 'Principles of Polymer Chemistry', Cornell University Press, Ithaca, NY, 1953
- 27 Richtering, W., Schatzle, J., Adams, J. and Barchard, W. *Colloid Polym. Sci.* 1989, **267**, 568
- 28 'Polymer Handbook' (Eds. J. Brandrup and E. H. Immergut), 3rd Edn., Wiley, New York, 1989
- 29 Mitchell, G. R. and Windle, A. H. in 'Developments in Crystalline Polymers-2' (Ed. D. C. Bassett), Elsevier, London, 1988, p. 115
- 30 Mitchell, G. R. in 'Comprehensive Polymer Science' (Ed. G. Allen), Pergamon, Oxford, 1989, Vol. 1, Ch. 31, p. 687
- 31 Fox, T. G. *Bull. Am. Phys. Soc.* 1956, **1**, 123
- 32 Guo, W., Davis, F. J. and Mitchell, G. R. *Polym. Commun.* 1991, **32**, 268
- 33 Finkelmann, H., Kock, H. J., Gleim, W. and Rehage, G. *Makromol. Chem., Rapid Commun.* 1984, **5**, 287
- 34 Barnes, N. R., Davis, F. J. and Mitchell, G. R. *Mol. Cryst. Liq. Cryst.* 1989, **168**, 13
- 35 Davis, F. J. and Mitchell, G. R. *Polym. Commun.* 1987, **28**, 8
- 36 Meier, W. and Finkelmann, H. *Makromol. Chem., Rapid Commun.* 1990, **11**, 599
- 37 Guo, W. and Mitchell, G. R. *Polymer* in press
- 38 Mitchell, G. R. *Polymer* to be submitted
- 39 Mitchell, G. R., Davis, F. J. and Guo, W. *Phys. Rev. Lett.* 1993, **71**, 2947
- 40 Bladon, P., Terentjev, E. M. and Warner, M. *Phys. Rev. (E)* 1993, **47**, 3838
- 41 Mitchell, G. R. in preparation